Precision in Assembled Discrete Lattice Space Structures for Next-Generation ISAM Applications

Christine E. Gregg
NASA Ames Research Center
Moffett Field, California 94035
christine.e.gregg@nasa.gov

Kenneth C. Cheung
NASA Ames Research Center
Moffett Field, California 94035
kenny@nasa.gov

***Abstract*— Robust autonomous robotic assembly of large-scale space structures has been a long-term and challenging goal to enable higher quality in-space communication and science instrumentation. For optical observatory support structures and antenna structures, the challenge is the strict dimensional precision requirements (generally RMS surface error) driven by the operational radiation wavelength. Early theoretical work in the area linked RMS surface error of a reflector support truss plate to the natural passive dynamic mode frequencies of the structure, as well as to the error distribution in dimensions of constituent structural elements. Prior robotic truss assembly demonstrations focused on designing ultra-high precision structural elements, joints, and robotic actuators. Recently, an alternative space structure assembly strategy based on a programmable matter approach (NASA ARMADAS) was demonstrated. This approach uses lattice building blocks (voxels) that are reversibly, mechanically joined into a bulk lattice structure by robots that locomote in and on the structure itself. Such a system can achieve high-level autonomy with low computation, robustly assemble utilizing inexpensive and imprecise robots, and efficiently build structures several orders of magnitude larger than the assembly robots. However, for instrumentation support structure applications, the resulting precision of these building block-based lattice structures is not well studied. Since they are demonstrated with many more assembly units than prior art trusses, it is unclear whether the same precision design approaches apply. In this work, we study in simulation the effects of voxel geometry, error distribution, assembly resolution (module size), and assembly geometry on the error of both beam and plate lattice structures. While average RMS error of a plate increases with plate size, increasing plate thickness quickly collapses RMS error towards a limit that is on the order of the error of the constituent parts. We validate our models against previously published precision measurements of built systems. Results from this study will guide manufacturing precision requirements, as well as designs, for future robotically assembled structural applications and establish feasibility for different applications.**

TABLE OF CONTENTS

1. INTRODUCTION

In-space assembly is a long-term capability goal for NASA and space agencies around the world due to its ability to circumvent the size, mass, and strength constraints on space structures imposed by launch vehicles. Decadal studies, NASA technical roadmaps, and the NASA's Moon to Mars objectives all identify science, technological, and exploration priorities (larger telescopes, lunar infrastructure) that challenge the capabilities of traditional deployable structures. Though past examples of in-space assembly included extensive astronaut assembly via EVA, the associated risk and time yielded consensus on the necessity of robotic assembly.

There are several proposed approaches to robotic structural assembly, with varying levels of autonomy. Many assembly operations on the International Space Station have been carried out using tele-robotic manipulation. However, as missions move to locations further from earth, signal delays and bandwidth limitations make tele-operation of robotics impractical, increasing the focus on efficient and robust fully autonomous systems. State of the art of robotic technology for in-space assembly of large structures is well reviewed by Dogget et al., and includes ground demonstration of assembly of struts and deployable modules[1]. The NASA In-Space Astronomical Telescope (iSAT) study identified key architectures and candidate technologies for assembling the next in-space observatory [2], arguing that next generation instrumentation will require assembly technology beyond the single-launch deployable paradigm. Tethers Unlimited SPIDERFAB technology combines in-space truss manufacturing with robotic emplacement [3] and will be tested on NASA OSAM-1, the first of multiple anticipated NASA missions to demonstrate In-Space Servicing, Assembly, and Manufacturing (ISAM) capabilities to meet future needs.

The NASA Autonomous Reconfigurable Mission Adaptive Digital Assembly Systems (ARMADAS) seeks to address challenges around autonomous robotic assembly by implementing a high-performance modular robotic assembly system rooted in programmable matter and discrete material concepts [4]. The system relies on high-performance discrete lattice building blocks (termed voxels) that are assembled by simple robots [5] [6] into large-scale structures. Since these robots locomote in and on the structure, they can leverage the precise structure for metrology and error correction [7]. In conjunction with alignment features on the structural modules, this not only decouples the precision of the structure from the precision of the robots, but also allows the robots to perform robust and fully autonomous assembly with very low perception, sensing, and computation requirements.

Though preliminary work demonstrates that this could be a scalable and robust way to produce high-performance lattices for primary structural support applications, evaluation of achievable structural precision associated with this methodol-

ogy has not been thoroughly investigated. Prior work showed that statistical and elastic averaging associated with discrete lattice structures could lead to increased precision in the 1-dimensional beam case (and consequently the hierarchical 2-dimensional case) [8], but this has yet to be extended robustly to generalized 2-dimensional, non-hierarchical structures.

2. BACKGROUND

Due to increased performance with increasing size, reflectors and antennas used for power transmission [9], communication, and scientific imaging are some of the highest value candidate structures for space assembly. These structures have stringent geometric precision requirements, since the surfaces of these reflectors need to be accurate within fractions of the wavelength at which they operate (typically 1/20th to 1/100th of a wavelength [10]). Meeting these precision requirements is very challenging, especially for optical applications, since manufacturing errors of both the surface and support structure, deployment errors, and assembly errors can all contribute to costly distortions that reduce the value of the asset (in addition to thermal distortions). For example, the surface of the Hubble Space Telescope originally had a manufacturing error that lead to an out of specification reflector surface that required costly repair missions. Though the primary support structure of optical elements is several orders of magnitude less precise than the optical surface, the ability to control and predict surface error is key for the operation of shape correction hardware to meet extreme accuracy requirements of optical systems [10].

Accordingly, the achievable precision of assembled tetrahedral truss structures due to part precision has been explored analytically, computationally, and experimentally. Hedgepeth presented an analytical argument that RMS surface accuracy should be proportional to the sum of the inverse square of structural fundamental frequencies [11]. Greene extended this work through simulation and related expected RMS accuracy of tetrahedral trusses to the number of rings in a the truss [12]. Wu et al. designed and assembled a 8m flat tetrahedral truss structure that achieved 0.0055 inch RMS surface error using members and nodes with precision on the order of $\pm$ 0.002 inch [13]. Greene and Hafka simulated the same 8m truss and reported a similar RMS surface error result (0.0023 inches), and they also note a method by which member exchange can be used to reduce RMS error and residual stress in the resultant truss. Bush et al. designed and assembled a 4m doubly curved tetrahedral truss structure that achieved an RMS surface accuracy of 0.003 in. using struts with an a tolerance of $\pm$ 0.0002 in [14]. These studies provide thorough grounding of design principles and experimental validation for the tetrahedral truss, but do not sufficiently explore alternative truss geometries like those proposed by the ARMADAS project and discrete materials literature. Hogstrom explores the effect of different error types in detail throughout the assembly process for structural modules for a telescope backbone [15]. Similar to prior work on tetrahedral trusses, we wish to extend these methodologies to geometries of the discrete lattice materials considered in the ARMADAS project.

Discrete materials, also known as digital materials (not for their electrically active properties but for their discrete 'bit' like composition and fungability), are physical material systems that are composed of many interchangable building blocks. The digital materials paradigm, as well as the related fields of programmable matter, seeks to extend the advantages of the digital computation (perfect replication in noisy environment, precision over millions of replications, etc.) to the current, inherently analog, process of manufacturing and material processing.

Digital material precision literature has shown that careful design of assembled parts can lead to assemblies which are more precise than their constituent parts, due to elastic averaging and statistical effects. Slocum and Weber use the principle of elastic averaging to design a passive mechanical wafer alignment technique capable of greater than micron alignment accuracy [16]. The authors note that elastic averaging "assumes the system is grossly over constrained, but each contact element is relative flexible, and when forces are applied to clamp the system, the elements deform elastically and errors average" [16]. To investigate the repeatability of elastic averaging, the authors study assemblies of Lego™ Duplo™ blocks, which can be understood as digital assembled materials. Their results demonstrate that both repeatability (sub-micron) and standard deviation improved as the number of contact points increased (number of blocks). Therefore, it is theoretically possible (though not guaranteed depending on attachment design) that assemblies of digital materials can be more precise with increasing number of elements. Hints of this counter-intuitive result are seen in traditional space structure literature by Greene [12], who noted adding rings to tetrahedral trusses (increasing elements and constraint) resulted in improved precision. Hiller and Lipson also studied the precision of 1D, 2D, and 3D sphere and tile voxel assemblies, noting sublinear scaling of error with assembly size [17].

3. METHODS

We wish to understand the precision of assembled discrete lattice systems with random error from manufacturing or assembly. For this work, we consider lattices of the cuboctahedron geometry (Fig. 1) [18], [19] since it is of interest for autonomously assembled lattice systems due to its combination of strength, stiffness, and relative ease of assembly [20], [21], [22].

To simulate the effect of manufacturing error on the overall precision of discretely assembled lattice systems, we simulate random error in the strut lengths of each assembly using a method first suggested by Greene [10] and used in Jenett 2017 [8]. This assumes that each voxel is manufactured and assembled using a 'strut and node' methodology, where each strut length is independently manufactured and connected at the nodes to form voxels. The model assumes perfect rigid connections between the voxels, a modeling assumption that is well supported by experimental examples that feature preloaded, bolted joints that are much more stiff than the struts [19] (which can be typical for ultralight discrete lattices). Analysis of systems featuring joints with stiffness on the order of the struts would need to more accurately model such interaction (example provided in validation portion of this work). Two different types of voxel decompositions are considered: node connected octahedra and face connected cuboctahedra (Fig. 1). These two different voxel unit cell options end up producing the same bulk lattice geometry when tiled. However, since the cuboctahedra are connected along faces instead of struts, they contain 'doubled struts' on interior voxel interfaces, which are two parallel struts adjacent or abutting one another and lying in the same plane. The double strut geometry is treated separately from single strut geometry due to differing constraints to understand

potential differences in error behavior due . Many physical instantiations of the cuboctahedron decomposition are possible, each of which might have different detailed models. We evaluate this preliminary simplified 'double coincident strut' model to isolate the potential contribution of differing constraints along boundary layers and interior layers, even if it is non-physical in many ways.

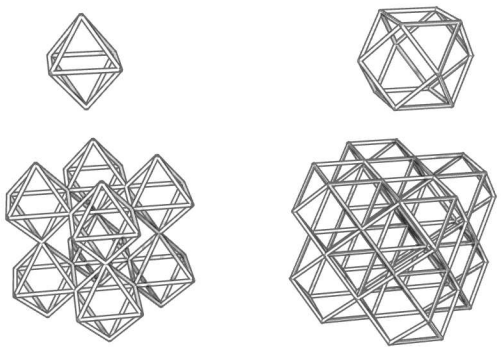

Figure 1. Two decompositions of the cuboctahedral lattice are considered: vertex connected ocahedra (left) and face connected cuboctahedron (right).

We consider two generalized structures of interest for most space applications (Fig. 2). The first is a structure with extents primarily along a single dimension, also known as a beam, such as a boom or interferometer structure. The other is a structure with extents primarily along two dimensions, also known as a plate, often used as support structure for reflectors or solar panels. Though such structures have many structural requirements (dynamic, thermal, etc.), we consider here static primary structural precision measures: length for beams and RMS flatness for plates.

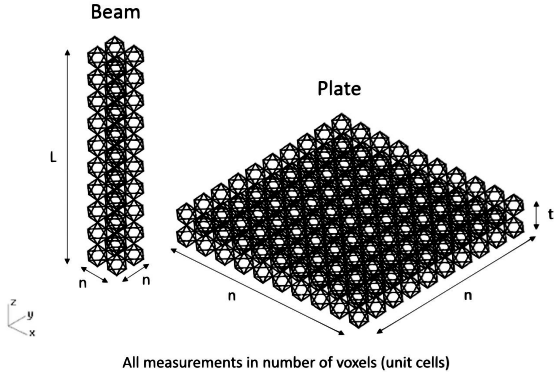

Figure 2. Beams had a cross-section of n by n voxels, with a length of L voxels, where L is much greater than n. Plates had an area of n by n voxels and a thickness of t voxels, where n is much greater than t.

Simulations

For this initial work, we simulate the effects of manufacturing errors as either a random Gaussian or uniform distribution of length error for each strut in the assembly. In the finite element simulation, this variation in length is achieved by applying a random value of thermal expansion to each beam in the assembly (centered at zero with a prescribed standard deviation) and simulating a unit temperature increase. We use this thermal expansion approach not because we are studying thermal distortion effects, but because doing so allows us to test many different samples of simulated error, from as many distributions as desired, all on the same finite element model. This methodology allows simple enforcement of lattice node network connectivity for a network of randomized length struts without needing to rebuild the finite element model for each sample of strut lengths, leading to significant time and effort savings to study the effect of manufacturing precision. Studying distortions due to thermal effects would require a different modeling approach. Randomization is conducted in Java using the SecureRandom object, which offers a 128-bit pseudorandom number that is sufficient for the assembly sizes considered in this work (<100,000 elements). As previously explained, the cuboctahedron voxel assemblies contain 'doubled struts' along interior voxel interfaces. In simulation, these doubled struts are modeled as coincident, which we should emphasize does not correspond to physical reality, but is sufficient for the purpose of this work. Each strut, doubled or otherwise, was modeled as 4 ABAQUS B31 beam elements. In the following methodology, a 'strut' refers to all of the elements in a lattice edge.

This methodology is taken from our previous work in [8] and reproduced here for completeness. Each voxel component is assumed to be randomly selected from a population of parts with normally distributed lengths of a known mean μ and standard deviation θ. We assign a random length error e to each truss element. If the nominal truss strut length is L^*, then

$$Error = e = L - L^* \tag{1}$$

where L is the observed length of the strut. This can be conceptually transformed into an equivalent random initial strain in each truss element [10].

$$\epsilon_i = \frac{L - L^*}{L^*} = \frac{e}{L^*} \tag{2}$$

Since the error is normally distributed about an average with a given standard deviation σ_e, then for a 99 percent confidence interval, the initial strain can be written as

$$\epsilon_i = \frac{\bar{e} \pm 2.58\sigma_e}{L^*} = \bar{\epsilon_i} \pm 2.58\sigma_{\epsilon_i} \tag{3}$$

In our case, the average of the error is zero (error equally likely to be negative and positive). Thus the initial strain is also centered about zero.

To achieve this strain in simulation, we apply a random orthotropic thermal expansion along the beam length (coefficient of thermal expansion is zero in the plane of beam cross-section, non-zero along the beam axis, commensurate with the simulated length error). We know that the strain of thermal expansion is dependent upon the coefficient of thermal expansion α and the change in temperature ΔT:

$$\epsilon_T = \alpha \Delta T \tag{4}$$

If the coefficient of thermal expansion is distributed about an average with a given standard deviation σ_α, it can be shown that

$$\epsilon_T = (\bar{\alpha} \pm 2.58\sigma_\alpha)\Delta T = \bar{\epsilon_T} \pm 2.58\sigma_{\epsilon_t} \tag{5}$$

By equating the thermal strain and the desired initial strain, it can be shown that

$$\sigma_{\epsilon_i} = (\sigma_\alpha)\Delta T = \frac{\sigma_e}{L^*} \tag{6}$$

Each strut is assigned a random coefficient of thermal expansion taken from a distribution with a given standard deviation. As shown in Eqn. 6, this coefficient of thermal expansion translates to a initial strain representing a manufacturing length error. One dimensional beam simulations have a encastre boundary condition at the base of the lattice beam and extend in the z direction. The deformed beam length is calculated as the average resultant z coordinate of all nodes at the end of the beam. Error is reported as delta, the difference between the deformed length and nominal length, normalized by the nominal length.

Two dimensional plate simulations were modeled with one corner node of plate fixed, to allow for unconstrained deformation of the surface. The RMS surface error was calculated by fitting a flat plane to the deformed surface nodes and then calculating the RMS error between the surface nodes and the fit plane. The octahedra had one surface node per voxel, while the cuboctahedron used all corner nodes along the top surface. Subsampling surface nodes for the RMS calculation was shown to have negligible effect on the RMS surface calculation (Appendix B). Unless otherwise noted, the constituent material was modeled as RTP2187, which has a modulus of 4.9e6 psi (33 GPa). Strut STD values are presented as error distribution STD as a percentage of strut length (unless otherwise noted with absolute length units).

4. RESULTS

Figure 3 shows the average error for beams of different voxel cross-sections and lengths. The voxel material was RTP2187 and the pitch was 3 inches, to match a previously published example of cuboctahedron discrete lattice constructed from vertex connected octahedra [19]. Error in beam length decreases both with voxel cross section and beam length, which supports trends first noted in [8].

Figure 4 shows the average RMS surface error of different sized plates using the same 3 inch voxels. Results show that while error increases with increasing plate size, error decreases to a threshold level with increasing plate thickness. The same trend is observed with the variability of the RMS error, an expected result of elastic averaging also observed in prior art. Equivalently sized octahedra and cuboctahedron voxels demonstrate similar trends with increasing plate size and thickness (Figure 5). Both approach similar RMS error limits, with the octahedra version showing slightly better error at high plate thickness. Interestingly, the octahedra is not always more precise that the cuboctahedron, especially at low thickness. The cuboctahedron geometry shows much faster convergence toward an ultimate precision limit. Both of these differences are attributed to the differences in constraint of the surface nodes of each voxel geometry. Distribution characteristics of the random error observed in a part population may depend on the manufacturing method and tolerances. Two different random distributions were studied, Gaussian and uniform. Using the same 3inch RTP2187 octahedra voxels, Figure 6 shows a comparison between a Gaussian distribution with a standard deviation of 0.1 percent of strut length and a uniform distribution that was +/- 2 standard deviations (covering approximately 95 percent of the Gaussian

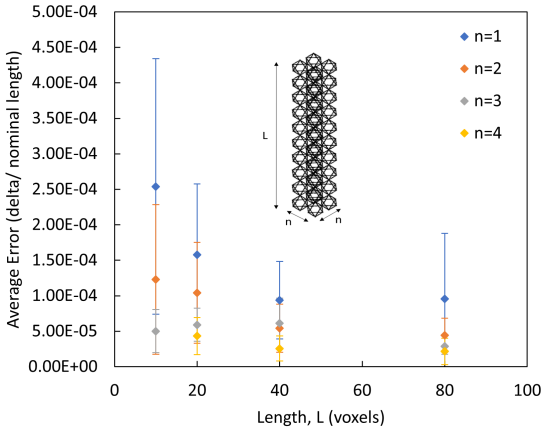

Figure 3. Average error of beam length (delta=deviation from nominal length) for different sized beams measuring n × n × l voxels. Voxel pitch was 3 inches, beam width 0.05 inches (square cross section), strut length error was a Guassian distribution with a STD of 0.001, and material stiffness was 33GPa. Error bars show one standard deviation (N=10).

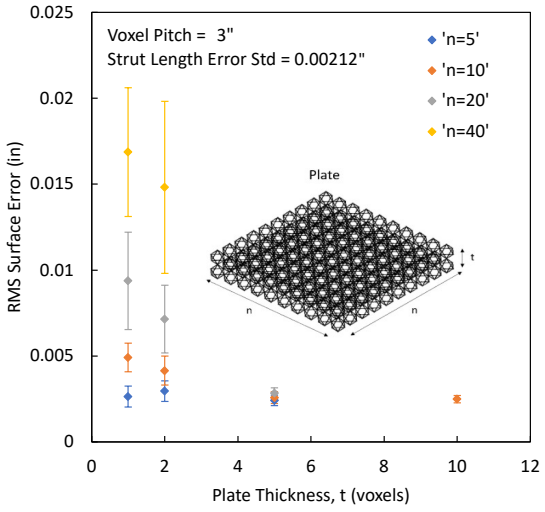

Figure 4. RMS surface error for different sized plates measuring n × n × t voxels. Voxels have a 3in pitch to match a previously published example of cuboctahedron discrete lattice constructed from vertex connected octahedra [19]. Error bars show one standard deviation (N=10).

distribution range in the ideal case). Both distributions follow the same trend of decreasing RMS error with plate thickness, approaching similar limits. To directly compare the effect of different levels of voxel resolution on the precision of a plate of a given size, equal mass plates of octahedra voxels were compared with two different levels of resolution (Figure 7). Two different sizes were used, 12 inches and 6 inches, with the beam width and error distribution of each adjusted so that they had equal relative density and struts of equal absolute precision (Appendix A). Results in Figure 8 show that higher resolution confers no significant penalty, and at large plate size and thicknesses, can even confer modest advantages.

Figure 9 shows the isolated effects of changing the standard

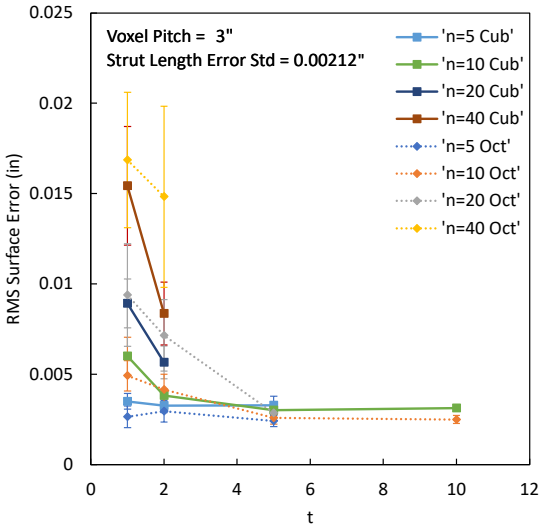

Figure 5. RMS surface error for different sized plates measuring n × n × t voxels, constructed from vertex connected octahedra (beam width = 0.05 inch) and face connected cuboctahedron (beam width = 0.025 inch). Cuboctahedron voxels had beam widths half those of the octahedra to account for strut doubling along interior faces. Material modulus was 33 GPa. Error bars show one standard deviation (N=10).

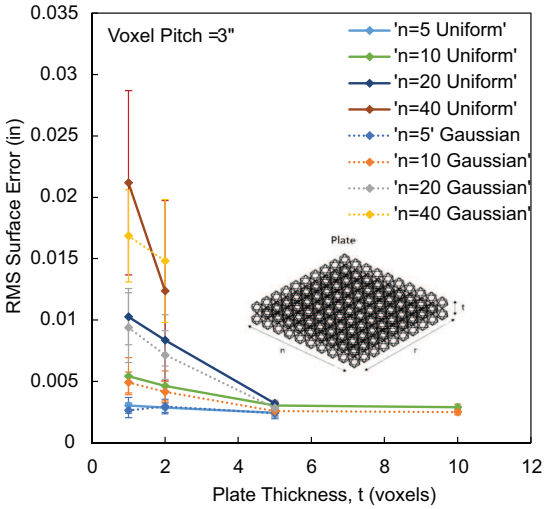

Figure 6. Gaussian vs. uniform distribution. The uniform distribution is assumed to be +/- 2 standard deviations of the Gaussian distribution. Error bars show one standard deviation (N=10).

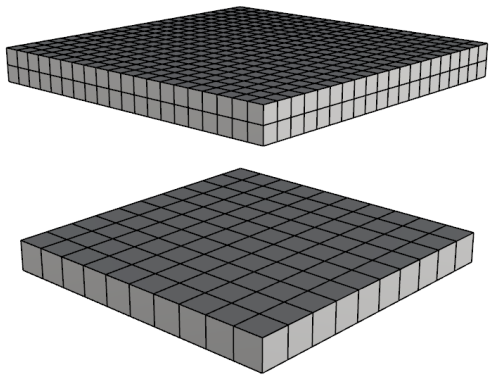

Figure 7. Plates of equal size, different voxel resolution.

deviation of the strut error distributions and the material stiffness on the RMS surface error of a 20x20x2 plate assembly. Results show that the error distribution in the struts strongly influences the resultant RMS surface error (order of error is approximately the same as the order of surface error). Conversely, orders of magnitude change in the material stiffness shows a weak influence on overall RMS surface error. Both of these results agree with findings by Wu et al. [13]. Similar results were found for the effects of strut length error and material stiffness on the length error of a 2x2x20 unit cell beam assembly (Fig. 10).

Figure 11 shows results for 12 inch pitch octahedra voxels with an Gaussian error distribution with a standard deviation of 0.1 percent strut length. The plate sizes of 10, 20, 40, and 65 voxels represent 3m, 6m, 12m, and 20m class reflectors respectively. Results show that even at large scale, increasing the plate thickness can quickly reduce average RMS error to sub-millimeter scale.

To compare to literature values, we simulated a previously published 8m precision assembled planar truss structure (Figure 12) and compared the RMS surface error with experimental results [13], using an approximation of the error distribution of the members and nodes reported in [23]. Greene et al. [23] report a simulated RMS error of 0.0023 inches from an random arrangement of members and nodes, noted to be the same order as the error of the components. Wu et al. [13] simulated and assembled a different random arrangement of the same hardware, with a experimental RMS error of 0.0055 inches and simulated predicted error of 0.0043 inches (using the exact strut error arrangement used in the experiment). Our simulations yielded the same order of error, an average RMS of 0.0041 inches. This is in good agreement with the previously reported results given necessary approximation of distributions, since any single distribution of member lengths can yield a range of results. This also shows the extensibility of the modeling approach to include separate contributions of struts and nodes for future discrete lattice models with increased detail for given physical manufacturing approaches.

5. Discussion

The simulations in this work suggest that within limits, the precision of support plate structures for precision reflectors can be controlled by changing the thickness of the plate. Increasing thickness to meet a certain precision level clearly represents a proportional increase in system mass. Whether this increase is acceptable depends on various other mission design criteria. However, the ability of voxel material to be launched by multiple vehicles (including ride-along opportunities utilizing spare mass/volume of other missions), resuability, repairability, and extensibility of the system should all be considered when assessing mission cost and risk.

One advantage of using longer truss members and traditional

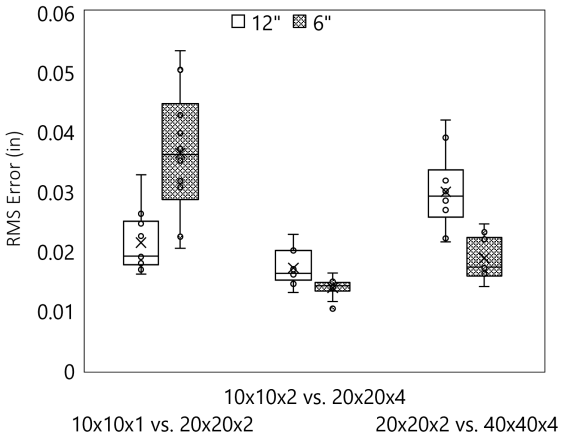

Figure 8. Equal sized, equal mass plates compared with different levels of voxel resolution. Twelve inch simulations were run with a beam width of 0.2, N=40, σ_α = 0.001. Six inch simulations were run with a beam width of 0.1, N=40, σ_α = 0.002. This is as an equal manufacturing tolerance with a standard deviation of 0.0085 in.

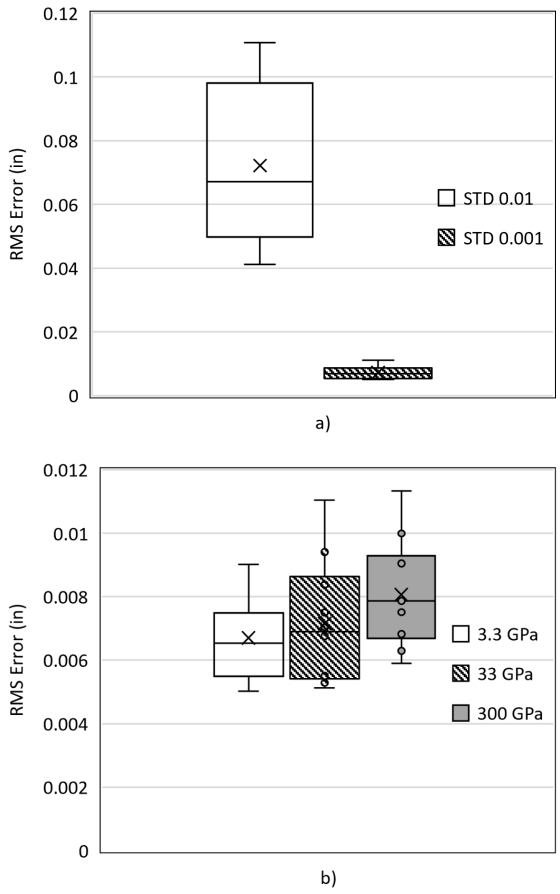

Figure 9. Isolated comparisons of the effect of material stiffness and error distribution standard deviation on error. All plates are 3inch octahedra, 20x20x2 unit cells in dimension, with 0.05 inch beam thickness, N=10. a) An order of magnitude difference in the standard deviation of the part error shows a strong influence on overall RMS surface error (roughly linear influence). b) Orders of magnitude change in material stiffness shows a weak effect on overall RMS surface error.

strut-node assembly like those in [14] is that for a prescribed manufacturing precision, the proportional member length error will be lower. This means that larger modules are functionally more precise with prescribed manufacturing tolerances than smaller modules made with similar tolerances. Achievable manufacturing tolerances are process and cost dependent. However, for high-end retail items, commercial machining (and therefore injection molding) processes can achieve unimodal normal distributions with 4 standard deviations within $\pm$ 0.03-0.05mm (0.001- 0.002 inch).

Our results are validated against the results of the 8m truss studied by Wu et al., which showed that RMS error tends to be on the order of the precision of the parts. It also showed that these types of simulations can be highly predictive of experimental results. However, subsequent results of a 4m parabolic truss show an order of magnitude less RMS precision than the constituent parts [14], suggesting potentially strong effects of plate geometry and joint design that should be explored in future work.

The results presented here use significantly simplified models; nevertheless, these models are still useful for the purposes of this work. While precise results for a specific lattice geometry require development of more accurate (and complex) models befitting the component unit cells, the overall trends and interactions observed in this work are products structural and physical interactions which are present in any digital material system. The validation work with the tetrahedral truss from Wu et al. demonstrated how, for strut and node construction, the error of the nodes (whether introduced by manufacturing error or slop in assembly) and struts can be separately accounted for. Additionally, if sections of the unit cell are manufactured monolithically [19], [24], those should likely be modeled as correlated errors. Despite the need for refinement when modeling a specific physical system, this work suggests that, in general, classical results can often be extended to discrete material systems. Also highlighted is the need to account for specific differences in geometry.

6. Conclusion

This work showed in simulation that increasing the number of unit cells in a beam assembly length and cross-section can increase the relative precision of the assembly. Similarly, though RMS surface error increases with increasing plate size, increasing plate unit cell thickness can quickly lower RMS surface error, while increasing the plate 'resolution' shows modest improvements in precision, attributed to the elastic averaging present in the parts. Material stiffness shows a weak influence on both beam and plate error measures, while the error distribution within the parts shows a strong influence. Simulations of traditional truss structures published in prior art validate the simulation methodologies and showed good agreement with previously published experimental data.

Experimental validation of these results is planned. We were not able to successfully measure the precision of injection molded octahedra [19] voxel examples because deviation between structures fell below the detection limit of the CMM machine used (likely due to high precision of injection molding process). To validate the behavior predicted by this work and reduce measurement requirements, we recommend use of

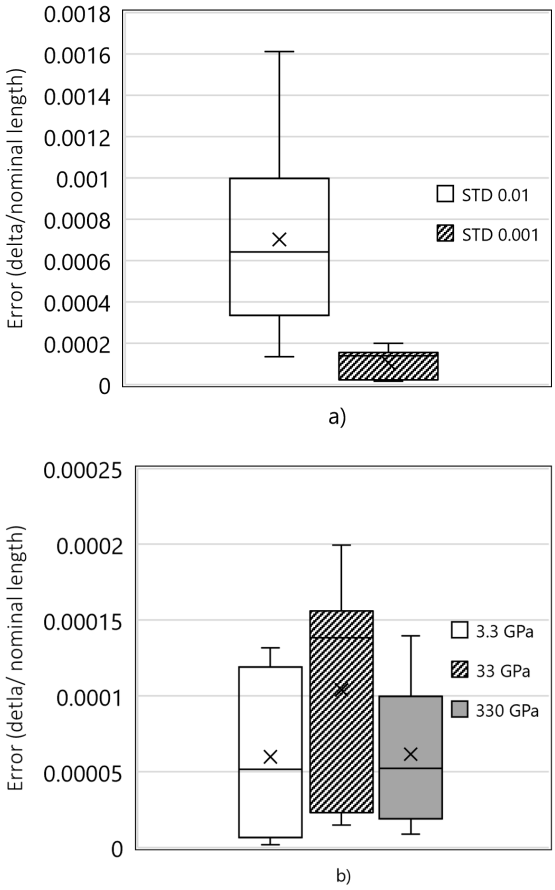

Figure 10. Isolated comparisons of the effect of material stiffness and error distribution standard deviation on error for beams. All beams are 3inch octahedra, 2x2x20 unit cells in dimension, with 0.05 inch beam thickness, N=10. a) An order of magnitude difference in the standard deviation of the part error shows a strong influence on overall length error (roughly linear influence). b) Orders of magnitude change in material stiffness show no appreciable effect on overall length error.

the largest unit cells that are practical, made with a relatively high error to validate predicted behavior. It is unknown how results from this study, which assume strut and node assembly, apply to other voxel manufacturing and assembly methods (eg. single part, stamped or molded cuboctahedra faces, or single part octahedra voxels), which might have different distributions of error that are uneven over the voxel dimension.

This work does not address hierarchical construction of reflector backbone surfaces. This analysis assumes solid filled plates, but we know that hierarchical truss structures (truss structures where the beams are themselves trusses) are more structurally efficient [8], [25], [26]. This work does also not address the question of assemblability and the strut prestress caused by dimensional errors. These topics were addressed for tetrahedral trusses by Greene [10] [23], but not for broader lattice and digital material assemblies. These and other precision considerations (dynamic effects, thermal effects) must be addressed for any given structure. However, understanding the effects of manufacturing tolerance is a key step towards understanding how to build scalable and precise

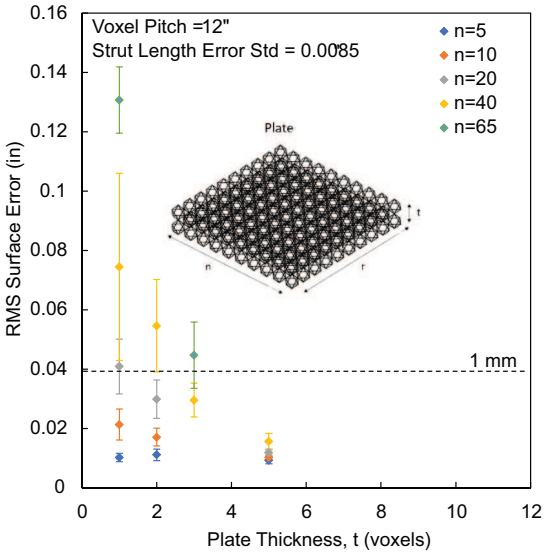

Figure 11. Twelve inch simulations were run with a beam width of 0.2, N=10, σ_α = 0.001. This is as an equal manufacturing tolerance with a standard deviation of 0.0085 in. The plate sizes of 10, 20, 40, and 65 voxels represent 3m, 6m, 12m, and 20m class reflectors respectively. Error bars show one standard deviation (N=10).

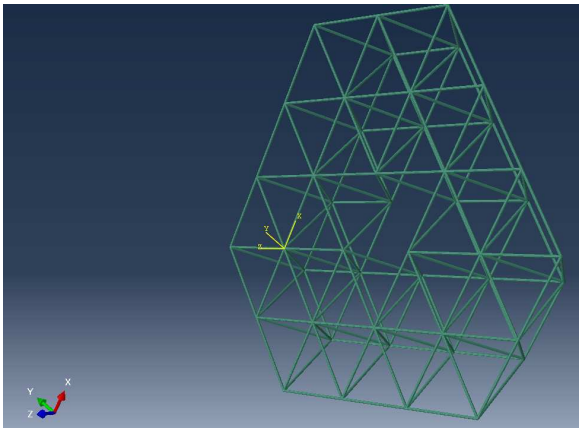

Figure 12. The 8m tetrahedral truss from Wu et al.[13] was simulated using published member length error distributions to validate current methodology.

discrete lattice structures.

APPENDICES

A. EQUAL MASS, EQUAL MANUFACTURING PRECISION CALCULATIONS

Relative Density Calculations

For comparison of plates with equal absolute dimensions but different levels of voxel resolution, it is crucial to compare structures with the same overall relative density (scaling down the length of voxel struts while proportionally scaling strut thickness). The idealized relative density, $\bar{\rho}$, which calculates the volume of square cross section struts and accounts for node volume by way of the spatial overlap of the struts, is

given by

$$\bar{\rho} = 3\sqrt{(2)}\left(\frac{t}{l}\right)^2 \tag{7}$$

where t is the strut thickness and l is the strut length. From this relationship, we can see that a lattice with twice the pitch (unit cell size) should have beams twice as thick to achieve equal relative density. For this comparison, we also wanted to have the same absolute strut error distribution. This modeled a fixed manufacturing precision used to manufacture parts of varying size. Say that we have two lattices, where the strut length of lattice two is twice that of lattice one ($L_2^* = 2L_1^*$). If we want the absolute length error to be equal between two lattices ($e_1 = e_2$), then combining Equations 2,3, and 6 yields the result that standard deviation of the coefficient of thermal expansion of the smaller lattice should be twice that of the larger lattice ($\sigma_{\alpha 1} = 2\sigma_{\alpha 2}$).

B. Effect of Subsampling on RMS

Testing of different spatial sampling frequencies had no discernible effect on the RMS calculation 13.

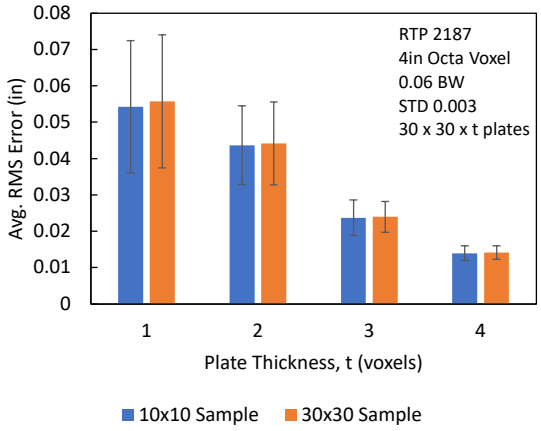

Figure 13. The effect of subsampling a large plate (30 x 30 surface nodes) at lower spatial sampling frequency (10 x 10) had no discernible effect on the RMS calculation for any thickness of plate.

Acknowledgments

This work was funded by NASA Space Technology Mission Directorate's Game Changing Development program (Automated Reconfigurable Digital Assembly Systems - ARMADAS). The authors gratefully acknowledge Dr. Chauncey Wu for providing invaluable information and insight.

References

[1] R. Doggett, J. T. Dorsey, and D. S. Kang, "State of the Profession Considerations: NASA Langley Research Center Capabilities and Technologies for Large Space Structures, In-Space Assembly and Modular Persistent Assets," Mar. 2021.

[2] R. Mukherjee, N. Siegler, and H. Thronson, "The Future of Space Astronomy will be Built: Results from the In-Space Astronomical Telescope (iSAT) Assembly Design Study," in *70th International Astronautical Congress (IAC)*, (Washington, D. C., United States), International Astronautical Federation (IAF), Oct. 2019.

[3] R. P. Hoyt, J. Cushing, and J. Slostad, "SpiderFab: Process for On-Orbit Construction of Kilometer-Scale Apertures," Final NNX12AR13G-FINAL, Tether's Unlimited, July 2013.

[4] C. Gregg, D. Catanoso, O. B. Formoso, I. Kostitsyna, M. Ochalek, T. Olatunde, I.-W. Park, F. Sebastianelli, E. M. Taylor, G. T. Trinh, and K. C. Cheung, "Ultra-light, strong, and self-reprogrammable mechanical metamaterials," *Science Robotics*, Jan. 2024.

[5] O. Formoso, G. Trinh, D. Catanoso, I.-W. Park, C. Gregg, and K. Cheung, "MMIC-I: A Robotic Platform for Assembly Integration and Internal Locomotion through Mechanical Meta-Material Structures," in *2023 IEEE International Conference on Robotics and Automation (ICRA)*, (London, United Kingdom), pp. 7303–7309, IEEE, May 2023.

[6] I.-W. Park, D. Catanoso, O. Formoso, C. Gregg, M. Ochalek, T. Olatunde, F. Sebastianelli, P. Spino, E. Taylor, G. Trinh, and K. Cheung, "SOLL-E: A Module Transport and Placement Robot for Autonomous Assembly of Discrete Lattice Structures," in *2023 IEEE/RSJ International Conference on Intelligent Robots and Systems (IROS)*, (Detroit, MI, USA), p. (In Press), Oct. 2023. (In Press).

[7] M. Carney and B. Jenett, "Relative Robots: Scaling Automated Assembly of Discrete Cellular Lattices," in *Proceedings of the ASME 2016 11th International Manufacturing Science and Engineering Conference. Volume 2: Materials; Biomanufacturing; Properties, Applications and Systems; Sustainable Manufacturing*, (Blacksburg, Virginia, USA), American Society of Mechanical Engineers, June 2016.

[8] B. Jenett, C. Gregg, D. Cellucci, and K. Cheung, "Design of multifunctional hierarchical space structures," in *2017 IEEE Aerospace Conference*, (Big Sky, MT, USA), pp. 1–10, IEEE, Mar. 2017.

[9] G. D. Convair, "Achievable Flatness in a Large Microwave Power Antenna Study," Final Report for Contract No. NAS9-15423 CASD-NAS-78-001, General Dynamics Convair Division, San Diego, CA, Aug. 1978.

[10] W. H. Greene, "Effects of random member length errors on the accuracy and internal loads of truss antennas," *Journal of Spacecraft*, vol. 22, no. 5, pp. 554–559, 1983.

[11] J. M. Hedgepeth, "Influence of fabrication tolerances on the surface accuracy of largeantenna structures," *AIAA Journal*, vol. 20, pp. 680–686, May 1982.

[12] W. H. Greene, "Effects of random member length errors on the accuracy and internal loads of truss antennas," *Journal of Spacecraft and Rockets*, vol. 22, pp. 554–559, Sept. 1985.

[13] K. C. Wu, R. R. Adams, and M. D. Rhodes, "Analytical and Photogrammetric Characterization of a Planar Tetrahedral Truss," NASA Technical Memorandum 4231, NASA, Hampton, Virginia, Dec. 1990.

[14] H. G. Bush, C. L. Herstrom, W. L. Heard, T. J. Collins, W. B. Fichter, R. E. Wallsom, and J. E. Phelps, "Design and fabrication of an erectable truss for precision segmented reflector application," *Journal of Spacecraft and Rockets*, vol. 28, pp. 251–257, Mar. 1991.

[15] K. Hogstrom, *Robotically Assembled Space Telescopes*

with Deployable Modules: Concepts and Design Methodologies. Doctor of Philosophy, California Institute of Technology, Pasadena, California, June 2016.

[16] A. Slocum and A. Weber, "Precision passive mechanical alignment of wafers," *Journal of Microelectromechanical Systems*, vol. 12, pp. 826–834, Dec. 2003.

[17] J. Hiller and H. Lipson, "Design and analysis of digital materials for physical 3D voxel printing," *Rapid Prototyping Journal*, vol. 15, pp. 137–149, Mar. 2009.

[18] K. C. Cheung and N. Gershenfeld, "Reversibly Assembled Cellular Composite Materials," *Science*, vol. 341, pp. 1219–1221, Sept. 2013.

[19] C. E. Gregg, J. H. Kim, and K. C. Cheung, "Ultra-Light and Scalable Composite Lattice Materials," *Advanced Engineering Materials*, vol. 20, p. 1800213, Sept. 2018.

[20] W. Chen, S. Watts, J. A. Jackson, W. L. Smith, D. A. Tortorelli, and C. M. Spadaccini, "Stiff isotropic lattices beyond the Maxwell criterion," *Science Advances*, vol. 5, p. eaaw1937, Sept. 2019.

[21] M. Ochalek, B. Jenett, O. Formoso, C. Gregg, G. Trinh, and K. Cheung, "Geometry Systems for Lattice-Based Reconfigurable Space Structures," in *2019 IEEE Aerospace Conference*, (Big Sky, MT, USA), pp. 1–10, IEEE, Mar. 2019.

[22] B. Jenett, A. Abdel-Rahman, K. Cheung, and N. Gershenfeld, "Material–Robot System for Assembly of Discrete Cellular Structures," *IEEE Robotics and Automation Letters*, vol. 4, pp. 4019–4026, Oct. 2019.

[23] W. H. Greene and R. T. Haftka, "Reducing distortion and internal forces in truss structures by member exchanges," *AIAA Journal*, vol. 28, pp. 1655–1662, Sept. 1990.

[24] B. Jenett, C. Cameron, F. Tourlomousis, A. P. Rubio, M. Ochalek, and N. Gershenfeld, "Discretely assembled mechanical metamaterials," *Science Advances*, vol. 6, p. eabc9943, Nov. 2020.

[25] T. Murphey and J. Hinkle, "Some Performance Trends in Hierarchical Truss Structures," in *44th AIAA/ASME/ASCE/AHS/ASC Structures, Structural Dynamics, and Materials Conference*, (Norfolk, Virginia), American Institute of Aeronautics and Astronautics, Apr. 2003.

[26] A. Vigliotti and D. Pasini, "Mechanical properties of hierarchical lattices," *Mechanics of Materials*, vol. 62, pp. 32–43, Aug. 2013.

BIOGRAPHY

Christine Gregg *received her B.S. in Mechanical Engineering from the University of Delaware and a Ph. D in Mechanical Engineering from UC Berkeley. She is a researcher at NASA Ames Research Center and most recently served as chief engineer on the ARMADAS project. Her research interests include space structures, robotic assembly, mission analysis, materials, and fracture mechanics.*

Kenneth Cheung *helps to run the NASA ARC Coded Structures Laboratory (CSL), which develops algorithmic structural systems and robotics to enable mission adaptive autonomous infrastructure for aeronautical and space applications. He is the Principal Investigator for the ARMADAS Project. As a member of the NASA ARC Intelligent Systems Division and affiliate of the office of the Center Chief Technologist, he serves as a technical lead on autonomy, robotics, advanced materials, and manufacturing. He received his Ph.D. from the Massachusetts Institute of Technology.*